Journal of Solid State Chemistry **144,** 461–466 (1999)
Article ID jssc.1999.8210, available online at http://www.idealibrary.com on IDEAL®

Effective Oxygen Content and Properties of $La_{0.74}Ca_{0.26}MnO_{3+d}$ as a Function of Synthesis Conditions

B. Dabrowski, P. W. Klamut,[1] Z. Bukowski,[1] R. Dybzinski, and J. E. Siewenie

Department of Physics, Northern Illinois University, DeKalb, Illinois 60115

Received November 10, 1998; in revised form January 26, 1999; accepted January 27, 1999

Using the thermogravimetric analysis measurements the effective oxygen content was measured for $La_{0.74}Ca_{0.26}MnO_{3+d}$ samples synthesized at high oxygen pressure. All samples were single-phase with orthorhombic, *Pbnm*, structure for the entire range of effective oxygen contents achieved, $0 \leq 3+d \leq 3.066$. The unit-cell volume decreases with increasing d, confirming that the holes are doped uniformly. The magnitoresistive transition temperatures increase intially with increasing effective oxygen contents but decrease for larger amounts of $d > 0.008$. Magnetic moment per Mn decreases with increasing d in agreement with the hole doping given by $h = x + 2d$. Structural and physical properties are consistent with the defect model of vacancies on the (La, Ca) and Mn sites in equal number, $v \sim d/(3+d)$. Results indicate that a small vacancy concentration on metal sites, $v < 0.003$, does not produce major structural or electronic effects other than the effective hole doping that increases T_c. For larger vacancy concentrations, scattering on defects may be a cause of observed decrease and broadening of T_c.

INTRODUCTION

Substituted $LaMnO_3$ materials are of considerable current interest owing to a large decrease of resistivity in a magnetic field near the Curie temperature, T_c (1). Classical theoretical models predict that the insulating state above T_c results from the spin scattering of e_g electrons (2, 3). Recent theoretical and experimental work has shown that additional localization may arise from a strong Jahn–Teller (JT) electron–phonon coupling that produces large oxygen displacements above T_c (4–10). These JT displacements are parallel to the Mn–O bonds and undergo considerable reduction below T_c for $La_{1-x}Ca_xMnO_3$ samples near $x = 0.22$ and 0.25 (11, 12). The strong dependence of resistivity, T_c, and structural properties on the average size, and the variance of sizes of the substituted alkaline and rare-earth ions in $LaMnO_3$ support a view of the powerful JT-electron–phonon coupling (13, 14).

[1]Also at the Institute of Low Temperature and Structure Research, Polish Academy of Sciences, P.O. Box 937, 50-950 Wroclaw, Poland.

The chemical stoichiometry that is a function of the synthesis conditions can also affect properties for lightly substituted samples, $x \leq 0.15$ (15–17). Research on pure and lightly substituted $La_{1-x}A_xMnO_3$ has shown that during synthesis under oxidizing conditions, large deviations from nominal stoichiometry are caused by the formation of vacancies on the metal sites A(La, Ca, etc.) and B(Mn) while the oxygen network remains undefected (16, 17). Using density measurements, structural studies by high-resolution electron microscopy and neutron powder diffraction, and thermodynamic considerations of defect models it was shown that vacancies on the A and B sites form in approximately equal amounts; i.e., $v \sim v_A \sim v_B \sim d/(3+d)$ (15, 17, 18). These results were supported by the observations that no impurity phases appear after synthesis in air or oxygen (11, 12, 15–20).

Most of the recent work on the moderately substituted materials, $0.15 < x < 0.30$, does not seem to delibrate on the variable chemical stoichometry since variety of synthesis conditions were employed ranging from annealing at high oxygen pressure at 650°C to annealing in air or argon at 1400°C followed by quenching or furnace cooling (19–21). No variation, or small variation of properties, was reported, but no quantitative measure of defects was given (20). Consequently, it is generally believed that samples near $x = 0.3$ always form stoichiometric (12, 20). We have recently shown that contrary to earlier assertions considerable nonstoichiometry and widely varying resistive and magnetic properties can be achieved under various synthesis conditions for $La_{1-x}Ca_xMnO_3$ samples with $x = 0.22$ (11). Since the phase diagrams are complex and very sensitive to hole concentration, it is, thus, of critical importance to report the proper material stoichiometry. Formation of vacant site defects in addition to a significant increase of the average Mn oxidation level, $h = x + 2d \sim x + 6v$, may also introduce large local oxygen displacements. Vacant Mn sites and oxygen displacements, located on the electronically active Mn–O network, can yield charge localization and other effects that may be incorrectly interpreted as resulting from the electron–phonon interactions.

0022-4596/99 $30.00

We report here a study of the effective oxygen content and structural, resistive, and magnetic properties of the $La_{0.74}Ca_{0.26}Mn_{3+d}$ sample prepared by the conventional solid-state ceramic method. Using high-sensitivity thermogravimetric analysis we have determined the effective oxygen content, $3 + d$, under several oxygen pressures and temperatures to 1400°C. Structural results obtained for the single-phase materials show that the orthorhombic, *Pbnm*, structure is formed for the whole range of effective oxygen content produced, $0 \leq 3 + d \leq 3.066$ (i.e., estimated vacancy concentrations, $0 < v < 0.022$). A decrease of the unit-cell volume with increased d confirms that additional holes are doped uniformly. Also, the magnetic moment per Mn decreases with increasing d in agreement with effective hole doping given by $h = x + 2d$. The magneto-resistive transition temperatures initially increase with increasing d, similar to substitution by Ca. However, despite further increase of the hole doping for larger amounts of effective oxygen content, $d > 0.008$, T_c's decrease probably because of the disorder on the Mn–O network. Structural and physical properties are consistent with the defect model of vacancies on the (La, Ca) and Mn sites in equal number.

EXPERIMENTAL DETAILS

A polycrystalline sample of $La_{0.74}Ca_{0.26}MnO_3$ was synthesized from stoichiometric mixture of the La_2O_3 (prefired in Ar at 700°C), MnO_2, and $CaCO_3$. The material was processed using the standard ceramic method and fired in air several times at various temperatures up to 1400°C followed by fast cooling to room temperature. The ceramic method leads to a low-density sample suitable for thermogravimetric measurements. The high-pressure annealing was done in pure oxygen (12 and 140 atm O_2) at 800°C. Crystal structure was studied by powder x-ray diffraction using a Rigaku powder diffractometer with Cu$K\alpha$ radiation. Magnetization and resistivity measurements were performed with a Quantum Design Physical Properties Measurement System. The effective oxygen contents were determined by thermogravimetric analysis measurements using a Cahn TG171 system with slow heating (2°/min) and cooling (0.6°/min) rates for ~1-g samples.

EFFECTIVE OXYGEN CONTENT

A series of $La_{0.74}Ca_{0.26}MnO_{3+d}$ samples with properties that are a function of the amount of the accurately measured effective oxygen content was prepared using the high oxygen pressure annealings and thermogravimetric analysis apparatus. To avoid additional complications, a composition $x = 0.26$ was chosen because the orthorhombic ($a \sim b \sim c/\sqrt{2}$) structure (12, 16) at room temperature should remain unchanged upon doping. Contrary to earlier reports (12, 20) the physical properties were very sensitive to the synthesis temperature and oxygen pressure. The high-resolution thermogravimetric measurements were used to correlate the varying properties with the effective oxygen content and to determine the synthesis conditions for stoichiometric sample.

Samples synthesized under various conditions in air at temperatures 1100–1400°C, on TGA in 100, 20, 1% O_2 and Ar, and in 12 and 140 atm O_2 at 800°C, were single-phase orthorhombic according to x-ray diffraction at room temperature. Absence of impurity phases that could contain remaining La, Ca, or Mn supports the notion that defects form as vacancies in approximately equal amounts on the A and B sites; i.e., we estimate that $v \sim d/(3 + d)$ for our samples (15–18). Thus, in the foregoing we will use this estimate to provide approximate amounts of vacancies for comparison with earlier data for $LaMnO_3$ and $La_{0.85}Sr_{0.15}MnO_3$ (18). However, if impurities have remained undetected and vacancies had formed in unequal amounts, our TGA data alone cannot provide a measure of each of v_{La}, v_{Ca} and v_{Mn} individually.

Two portions of a large (10 g) sample synthesized in air at 1400°C were annealed at 800°C for two days, using 12 and 140 atm O_2 and fast cooled to room temperature. Both parts were subject to two consecutive TGA runs. The part annealed at 140 atm was slowly heated to 1400°C and cooled to room temperature in 20% O_2/Ar gas mixture and then slowly heated to 1100°C and fast cooled to room temperature in pure Ar (~10 ppm O_2). The part annealed at 12 atm was slowly heated to 1400°C and cooled to room temparature in pure O_2 and then slowly heated to 1400°C and cooled to room temperature in 1% O_2/Ar gas mixture. To obtain a fixed point for the normalization of the oxygen content an additional TGA run was done in 50% H_2/Ar to 1300°C after heating in Ar. The TGA scan in 50% H_2/Ar showed a stable weight plateau above 750°C. X-ray diffraction of the reduced material revealed two phases, La_2O_3 and a mixed oxide, $Mn_{1-x}Ca_xO$. The observed weight loss in hydrogen was $\Delta d = 0.630 \pm 0.002$.

The oxygen content after heating in Ar at 1100°C was found to be 3.000 ± 0.002 per molecule of $La_{0.74}Ca_{0.26}Mn$. Figure 1a shows the TGA data for the starting material annealed at 140 atm O_2. The initial effective oxygen content is 3.066 ± 0.002. Assuming that vacancies form in approximately equal amounts on both metal sites A and B, we can estimate the vacancy concentration at $v \sim 0.022$. The large defect concentration may cause a significant increase of the doping level, $\Delta h = 2d \sim 6v \sim 0.13$, and, also, introduce local structural distortions and electronic inhomogeneity that could affect magnetic, transport, and structural properties.

The data on heating and cooling in 20% O_2 are almost fully reproducible at the temperature range 1050–1400°C ($\Delta d < 0.002$); i.e., the low-density sample is close to thermal equilibrium when slowly heated and cooled. On heating, the oxygen content is very close to 3.000 around 1300°C.

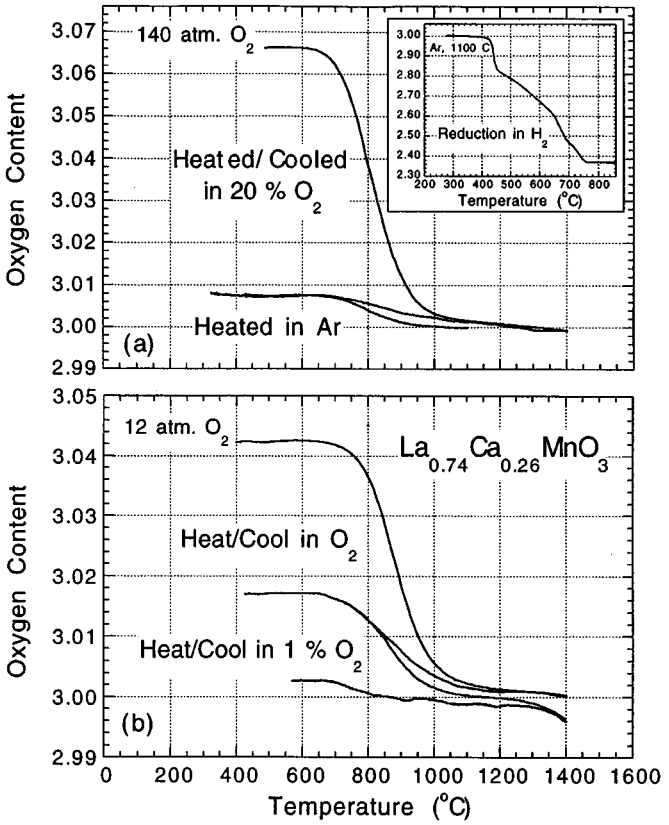

FIG. 1. Thermogravimetric analysis data for the low-density $La_{0.74}Ca_{0.26}MnO_{3+d}$ sample using (a) heating and cooling in 20% O_2 and heating in pure Ar (the starting materials have been annealed at 140 atm O_2) and (b) heating and cooling in 100 and 1% O_2 (the starting materials have been annealed at 12 atm O_2).

Oxygen content at 1400°C is slightly less than 3.000. On cooling down to 650°C, the oxygen content increases to 3.008 ± 0.002, i.e., $v \sim 0.003$, and the increase of the hole doping level is $\Delta h \sim 0.016$. No significant changes in oxygen content are seen below 650°C during either heating or cooling in 20% O_2. Also, heating in Ar at 1 deg/min does not change the oxygen content below 650°C. On heating in argon at higher temperatures, between 650 and 1000°C, the oxygen content gradually decreases to 3.000 and then remains unchanged during heating to 1100°C and the following hold for 10 h. An inset in Fig. 1a shows weight loss in hydrogen after heating in Ar.

Figure 1b shows the TGA data in 100 and 1% O_2 for the starting material annealed at 12 atm O_2. The normalization of the oxygen content to 3.000 was done at the center of an extended weight plateau near 1150°C in 1% O_2. The starting material has an effective oxygen content $3 + d = 3.042 \pm 0.002$; i.e., $v \sim 0.014$ and $\Delta h \sim 0.084$. The oxygen content decreases during heating in pure O_2 and is very close to 3.001 ± 0.002 around 1150–1400°C. On cooling down to 650°C, the oxygen content increases to 3.017 ± 0.002; i.e., $v \sim 0.006$ and $\Delta h \sim 0.034$. The oxygen content on heating and cooling at 100% O_2 is always larger than in 20 or 1% O_2 and is fully reproducible at the temperature range 1050–1400°C, showing that the sample is close to the thermal equilibrium. The oxygen content during heating in 1% O_2 shows a plateau from 1050 to 1250°C (used for normalization of the oxygen content by analogy to weight plateau in Ar) and decreases to 2.996 ± 0.002 at 1400°C. The effective oxygen content below 3.000 indicates the formation of vacancies on the oxygen network or slight decomposition of the material. On cooling, the oxygen content increases only slightly to 3.003 ± 0.002 at 650°C. The measured effective oxygen contents for all samples prepared by high-pressure annealing and on TGA apparatus are given in Table 1. The TGA data show that to make a stoichiometric $La_{0.74}Ca_{0.26}MnO_{3.00}$ sample an annealing in air at $\sim$1300°C (followed by quenching) in 1% O_2 at 1150°C or in argon at $\sim$1000°C should be used.

STRUCTURAL, MAGNETIC, AND RESISTIVE PROPERTIES

All samples prepared at high oxygen pressure and on TGA apparatus were characterized by powder x-ray diffraction at room temperature. Diffraction patterns could be indexed based on an orthorhombic unit cell with the space group *Pbnm*. Lattice parameters were calculated using the program DHN Powder Diffraction System (22). Figure 2 shows orthorhombic lattice parameters versus effective oxygen content, $3 + d$, obtained from the TGA data. The a and b lattice parameters decrease with increasing oxygen content similar to substitution by Ca. At the small values of effective oxygen content above 3 both a and b lattice parameters show a small anomaly. The c lattice parameter initially increases, has a maximum at $3 + d = 3.008$, and then decreases. It is unclear at present if the maximum of

TABLE 1

The Effective Oxygen Content ($\pm$ 0.002), Curie Temperatures [K], and Saturation Magnetic Moments [μ_B] ($\pm$ 0.004) for Samples Prepared by the High Pressure Annealing and on the TGA Apparatus

Sample	Oxygen content	T_c from $M(T)$	T_c from $R(T)$	μ_{sat}(exp)	μ_{sat}(calc)
Air, 1350°C, quenched	3.000	236	237	3.79	3.74
Ar, 1150°C, fast cool	3.000	263	NA	3.79	3.74
1% O_2, 1400°C, slow cool	3.003	237	239		
20% O_2, 1400°C, slow cool	3.008	241	246		
100%O_2, 1400°C, slow cool	3.017	236	239	3.73	3.71
12 atm O_2, 800°C	3.042	220	229	3.72	3.66
140 atm O_2, 800°C	3.066	185	188	3.60	3.61

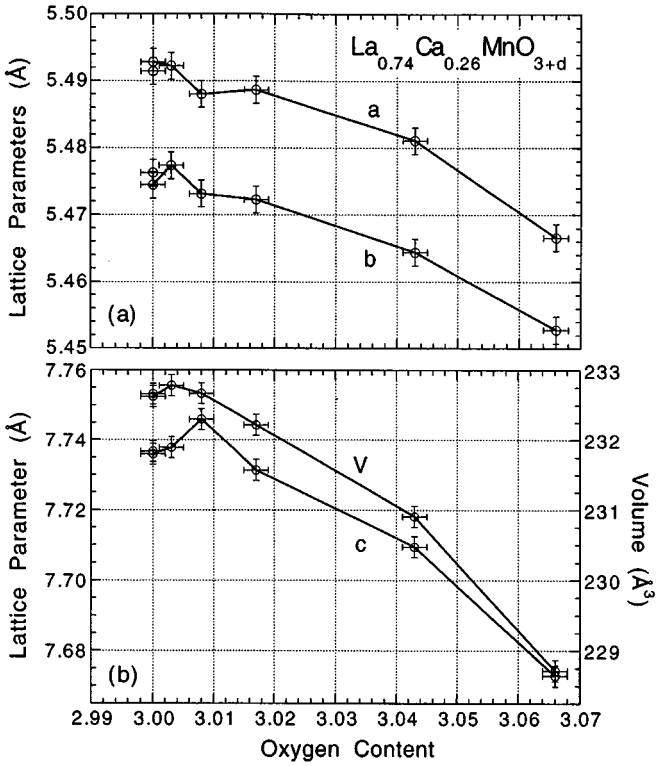

FIG. 2. Lattice parameters as a function of oxygen content obtained from TGA measurements for the $La_{0.74}Ca_{0.26}MnO_3$ samples using the orthorhombic *Pbnm* setting.

c and the anomalies of a and b lattice parameters are somehow related to the highest T_c of the sample cooled in 20% O_2. The unit cell volume shows a steady decrease with increasing effective oxygen content indicating that uniform doping of material is caused by a decrease of the ionic size of Mn on progressive oxidation to $3.26 + 2d$. The uniform doping of material suggests homogenous distribution of defects similar to that observed for pure $LaMnO_{3+d}$; i.e., it is consistent with the defect model based on random distribution of vacancies on A and B sites (15–18).

Normalized magnetization near the ferromagnetic transition at small magnetic fields is shown in Fig. 3a for several samples. Transitions are reasonably sharp for samples with small values of $d \leq 0.017$ ($v \leq 0.006$); slowly cooled on TGA in 20 and 100% O_2 and fast cooled in Ar. A similarly sharp transition was observed for the sample cooled on TGA in 1% O_2. That sample showed almost exactly the same transition as the sample cooled in 100% O_2 despite quite different effective oxygen content. A sample quenched in air from 1350°C ($d \sim 0$) showed a slightly broader transition indicating that it is difficult to preserve the stoichiometric composition during fast cooling for the low-density sample, probably because of the very fast oxygen and cation kinetics in air at high temperatures. Samples with larger amounts of effective oxygen content prepared at high oxygen pressures show gradually broader transitions. An increase of the ferromagnetic transition temperature can be observed with the initial increase of d. However, a larger amount of effective oxygen content, $d > 0.008$, leads to the suppression of transition temperatures. The accurate values of Curie temperatures were derived from the largest slope of the $M(T)$ curve and are included in Table 1.

Figure 3b shows the temperature dependence of magnetization for several samples in applied magnetic field of 3 T, i.e., a field high enough to achieve almost full saturation. The $M(T)$ curves show typical features for ferromagnets, i.e., shapes predicted approximately by the mean-field theory and increased transition temperatures in a magnetic field. The inset in Fig. 3b shows the magnetization as a function of the magnetic field in the vicinity of the saturation values at 6 K for samples with $d = 0$ (Ar annealed; data for the air-quenched sample gave almost exactly the same result),

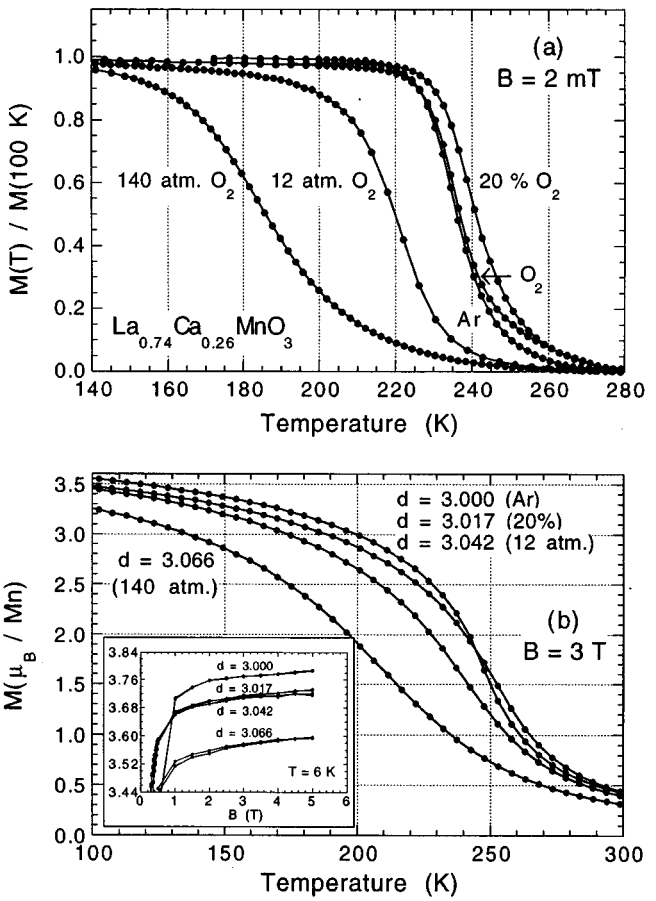

FIG. 3. (a) Normalized magnetization near ferromagnetic transition for several low-density $La_{0.78}Ca_{0.22}MnO_{3+d}$ samples cooled from 1400°C during the TGA measurements and annealed at high O_2 pressure at 800°C. (b) Magnetization near ferromagnetic transition in applied magnetic field of 3 T for samples with $d = 0$ (Ar annealed), 0.017, 0.042, and 0.066. (inset) Magnetization as a function of magnetic field in the vicinity of the saturation values of 6 K.

0.017, 0.042, and 0.066 ($v = 0$, 0.003, 0.014, and 0.022). The saturation magnetic moments, μ_{sat}(exp), were taken at a field of 5 T as fully saturated magnetization calculated per Mn ion. These average μ_{sat}(exp) are listed in the Table 1 and are compared with the theoretical saturation magnetic moments, $\mu_{sat}(\text{calc}) = (1 - x - 2d)\mu_{sat}(Mn^{3+}) + (x + 2d)\mu_{sat}(Mn^{4+})$, where $\mu_{sat} = 4\mu_B$ and $3\mu_B$ for Mn^{3+} and Mn^{4+}, respectively. The experimental values for μ_{sat}(exp) (measured with the accuracy of $\pm 0.04\mu_B$) decrease monotonically with increasing d, confirming the increased hole doping (increased Mn^{4+}/Mn^{3+} ratio) and show good agreement with the calculated values μ_{sat}(calc) (16). Magnetic measurements at high magnetic fields confirm, thus, good homogeneity of all samples and uniform doping consistent with a formula $h = x + 2d$.

Figure 4 shows the resistivities for several samples with small effective oxygen content, $d \leq 0.008$ (Fig. 4a), and with larger effective oxygen content, $d \geq 0.008$ (Fig. 4b). Transition temperatures T_c, inferred from the maximum of $R(T)$ (listed in Table 1), increase with the initial increase of d (Fig. 4a) and then decrease for larger amounts of effective oxygen content (Fig. 4b) in perfect agreement with magnetization data when transitions are sharp. The transition width is the sharpest for the nearly stoichiometric sample quenched in air from 1350°C, denoted (air). Transition widths gradually increase with increasing effective oxygen content probably because of disorder. When transitions are broad, resistivity shows generally higher T_c than magnetization. The broadening of resistive transitions could be more adequately described in terms of vacancies on the La and Mn sites and corresponding defects on the electronically active Mn–O network. It appears that the small amount of vacancies, $v \sim 0.003$, for the sample obtained on TGA in 20% O_2, acts mostly as the effective hole doping that increases T_c similar to an additional substitution by Ca. Larger amounts of vacancies depress T_c, probably due to increasing disorder despite a further increase of the hole doping. The number of defects sufficient to suppress T_c are surprisingly small for $x = 0.26$.

The absolute values of resistivity correlate well with the changes of T_c. Samples with small amounts of effective oxygen content and lightly increased hole doping have the lowest resistivity. The magnitude of resistivity initially decreases with increased doping similar to that observed with Ca substitution at this doping range. However, samples with large d and highly increased hole doping have higher resistivity, probably because of the increased electron scattering on defects. The decomposed material at the grain boundaries may be the cause of notably increased resistivity and a very broad transition for the Ar-annealed sample (23). The high grain-boundary resistance of the Ar-annealed sample makes the ferromagnetic transition at 236 K barely visible and results in apparent decoupling of the ferromagnetic and metal–insulator transitions. The grain boundaries

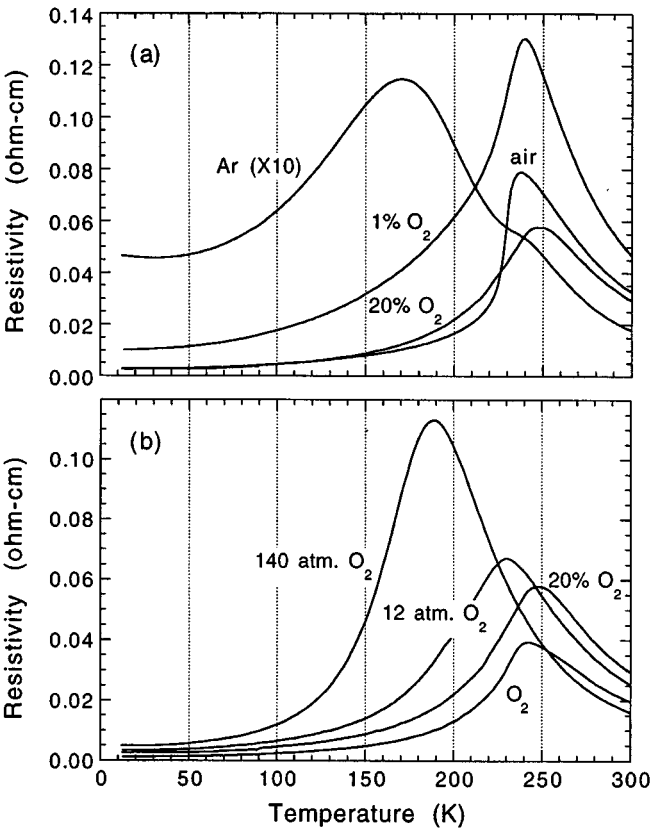

FIG. 4. Resistivity for several low-density $La_{0.78}Ca_{0.22}MnO_{3+d}$ samples: (a) quenched in air from 1350°C, fast cooled in Ar from 1150°C, and slowly cooled from 1400°C during the TGA measurements in 1 and 20% O_2; (b) annealed at high O_2 pressure at 800°C and slowly cooled from 1400°C during the TGA measurements in 100 and 20% O_2.

may also contribute to somewhat increased resistivity for the sample cooled in 1% O_2.

CONCLUSION

Pure and lightly substituted $LaMnO_{3+d}$ materials are known to accommodate considerable nonstoichiometry in the form of vacancies on the metal sites A(La, Ca, etc.) and B(Mn) in approximately equal amounts (15–18). We have shown that by using annealings at high and moderate oxygen pressure a substantial nonstoichiometry can be generated also for the moderately substituted $La_{1-x}Ca_xMnO_{3+d}$ samples with $x = 0.26$. Thermogravimetric analysis measurements provide sensitive measure of the effective oxygen content; i.e., assuming equal numbers of vacancies on the A and B sites, the vacancy concentration can be determined very accurately. The absence of impurity phases, uniform decrease of the orthorhombic unit cell volume, and monotonic decrease of saturated Mn magnetic moment with increasing effective oxygen content support the conjecture that defects form as vacancies in approximately equal

amounts on the A and B sites. The magnetoresistive transition temperatures increase initially with increasing effective oxygen content but decrease for larger $d > 0.008$. This effect when discussed in terms of defects on cation sites would indicate that small vacancy concentration on metal sites, $v \leq 0.003$, does not cause major electronic effects other than the effective hole doping. For larger vacancy concentration, local distortions and scattering on defects may lead to suppression and broadening of T_c. We have observed a similar effect previously for $x = 0.22$ at $d \sim 0.021$ ($v \sim 0.007$) (11). It appears, thus, that the amount of defects that can be allowed in the lattice without suppression of T_c depends on the initial substitution level x. Knowledge of the change and broadening of T_c by defects can be used to delibrately adjust transition temperature and its width to optimize the colossal magnetoresistive effect.

ACKNOWLEDGMENT

This work was supported by the ARPA/ONR.

REFERENCES

1. R. M. Kusters, J. Singelton, D. A. Keen, R. McGreevy, and W. Hayes, *Physica B* **155,** 362 (1989).
2. C. Zener, *Phys. Rev.* **82,** 403 (1951).
3. P. W. Anderson and H. Hasegawa, *Phys. Rev.* **100,** 675 (1995).
4. A. J. Millis, P. B. Littlewood, and B. I. Shraiman, *Phys. Rev. Lett.* **74,** 5144 (1995).
5. A. J. Millis, B. I. Shraiman, and R. Mueller, *Phys. Rev. Lett.* **77,** 175 (1996).
6. H. Roder, J. Zhang, and A. R. Bishop, *Phys. Rev. Lett.* **76,** 1356 (1996).
7. Y. Okimoto, T. Katsufuji, T. Ishikawa, A. Urushibara, T. Arima, and Y. Tokura, *Phys. Rev. Lett.* **75,** 109 (1995).
8. J.-S. Zhou, J. B. Goodenough, A. Asamitsu, and Y. Tokura, *Phys. Rev. Lett.* **79,** 3234 (1997).
9. D. Louca, T. Egami, E. L. Brosha, H. Roder, and A. R. Bishop, *Phys. Rev. B* **56,** R8475 (1997).
10. C. H. Booth, F. Bridges, G. H. Kwei, J. M. Lawrence, A. L. Cornelius, and J. J. Neumeier, *Phys. Rev. Lett.* **80,** 853 (1998).
11. B. Dabrowski, Z. Bukowski, X. Xiong, K. Rogacki, P. W. Klamut, R. Dybzinski, J. E. Siewenie, C. W. Kimball, and J. D. Jorgensen, unpublished.
12. P. G. Radaelli, G. Iannone, M. Marezio, H. Y. Hwang, S-W. Cheong, J. D. Jorgensen, and D. N. Argyriou, *Phys. Rev. B* **56,** 8265 (1997).
13. H. Y. Hwang, S-W. Cheong, P. G. Radaelli, M. Marezio, and B. Batlogg, *Phys. Rev. Lett.* **75,** 914 (1995).
14. L. M. Rodriguez-Martinez and J. P. Attfield, *Phys. Rev. B* **54,** R15622 (1996).
15. J. A. M. Van Roosmalen, E. H. P. Cordfunke, R. B. Helmholdt, and H. W. Zandbergen, *J. Solid State Chem.* **110,** 100 (1994).
16. J. Toepfer and J. B. Goodenough, *Chem. Mater.* **9,** 1467 (1997).
17. J. A. M. Van Roosmalen and E. H. P. Cordfunke, *J. Solid State Chem.* **110,** 106 (1994).
18. J. A. M. Van Roosmalen and E. H. P. Cordfunke, *J. Solid State Chem.* **110,** 109 (1994).
19. M. Hervieu, R. Mahesh, N. Rangavittal, and C. N. R. Rao, *Eur. J. Solid State Inorg. Chem.* **32,** 79 (1995).
20. P. Schiffer, A. P. Ramirez, W. Bao, and S.-W. Cheong, *Phys. Rev. Lett.* **75,** 3336 (1995).
21. J. F. Mitchell, D. N. Argyriou, C. D. Potter, D. G. Hinks, J. D. Jorgensen, and S. D. Bader, *Phys. Rev. B* **54,** 6172 (1996).
22. M. Wolcyrz, W. Urbanik, S. Mazgaj, J. Matuszewski, M. Andruszkiewicz, and W. Paszkowicz, "Program DHN Powder Diffraction System."
23. N. Zhang, W. Ding, W. Zhong, D. Xing, and Y. Du, *Phys. Rev. B* **56,** 8138 (1997).